



Active correction of the tilt angle of the surface plane with respect to the rotation axis during azimuthal scan



M. Sereno, S. Lupone, M. Debiossac, N. Kalashnyk, P. Roncin *

Institut des sciences moléculaires d'Orsay (ISMO), CNRS, Univ. Paris-Sud, Université Paris-Saclay, Orsay F-91405, France

ARTICLE INFO

Article history:

Received 4 January 2016
Received in revised form 30 March 2016
Accepted 2 May 2016
Available online 10 May 2016

Keywords:

Grazing incidence
Surface science
Fast atom diffraction
Triangulation

ABSTRACT

A procedure to measure the residual tilt angle τ between a flat surface and the azimuthal rotation axis of the sample holder is described. When the incidence angle θ and readout of the azimuthal angle ϕ are controlled by motors, an active compensation mechanism can be implemented to reduce the effect of the tilt angle during azimuthal motion. After this correction, the effective angle of incidence is kept fixed, and only a small residual oscillation of the scattering plane remains.

© 2016 Elsevier B.V. All rights reserved.

1. Introduction

Surface studies using grazing incidence angles offer a high degree of surface sensitivity. This the case for X-rays [1], high energy electrons [2] and ions [3] as well as fast atoms [4,7]. In these techniques the angle of incidence is only few degrees. For most diffraction experiments, the required high positioning accuracy of the sample is provided with a goniometer but this is hardly compatible with sample transfer under UHV conditions and with high temperature needed for annealing. The real challenge appears when the structural information lies in an intensity variation during an azimuthal rotation of the surface such as in ion beam triangulation [3] and even more drastically in atom beam triangulation [5,6]. Ensuring stability of the incidence angle better than 0.1° requires active correction. We describe here a method designed for atom beam triangulation in a grazing incidence fast atom diffraction setup (GIFAD) that solves this issue.

2. Grazing incidence fast atom diffraction

Grazing incidence fast atom diffraction (GIFAD or FAD) has recently emerged as a new surface science technique with exclusive surface sensitivity and high structural resolution [8,9]. In this technique a beam of \sim keV atoms impinges the surface at incidence angles θ of about one degree and with a angular spread

(divergence) typically around 0.01° . When the beam is aligned with a low index crystal direction, diffraction can take place provided that the surface quality is good enough in terms of flatness and coherence length. The latter quantity is defined here as the mean separation between crystal defects. First observed on single crystals of wide band gap ionic insulators such as LiF [10,11], NaCl [12], GIFAD has been shown to be successful in measuring metal surfaces [13,14], semi-conductors [15,9] and even single layers of inorganic compounds [8] and organic molecules [5,16]. For surfaces of organic molecules, diffraction is not as sharp as for bulk crystal surfaces or inorganic layers probably due to the presence of a higher density of structural defects. Fortunately, the triangulation technique [3,5,6] easily reveals the alignment direction of the adsorbed molecules while the shape of the azimuthal profile gives hints on the detailed molecular assembly [5]. Even faint diffraction is enough to derive the lattice parameter of the molecular organization [5]. Also, it has been suggested [17,18] that azimuthal scans around channeling directions could be used to measure the range R_c of the interaction potential above the surface. This fundamental parameter can be very useful for quantitative analysis since it governs the length $L_T \sim R_c/\theta$ of the atom trajectory above the surface [17]. At high energies, selective sputtering of step edges is also sensitive to the crystallographic direction [19]. In addition, GIFAD has demonstrated pronounced intensity oscillations during layer-by-layer molecular beam epitaxy growth [20]. Following these oscillations during azimuthal rotation would allow a better uniformity of the layers. Ideally, these azimuthal scans should be performed without changing the angle of incidence. This turns out to be more difficult than expected. On one hand it is not

* Corresponding author.

E-mail address: philippe.roncin@u-psud.fr (P. Roncin).

straightforward to put a goniometer under UHV condition. On the other hand, sample transfer and rotation devices do not always allow for ultra-precise positioning of the sample. Most often the surface normal has a small residual tilt angle τ of about one degree with respect to the rotation axis. This is sufficient to prevent straight-forward application of purely azimuthal scan. When the control of both the azimuthal and incidence angle is motorized, an on-line correction can be performed and is described below.

3. The orbit of the specular spot

For each azimuthal angle, the plane of incidence is defined as the plane containing both the incident beam and the surface normal. It also contains the specularly reflected beam, so that the location of the specular beam on the detector indicates the direction of the surface normal. During an azimuthal scan the specular beam spot follows a curve that can be described as an orbit. Using the standard description of specular scattering,

$$\vec{k}_{spec} = \vec{k}_{in} - 2(\vec{k}_{in} \cdot \vec{N})\vec{N} \quad (1)$$

where $\vec{k}_{in} = -k_0\vec{x}$ is the incoming wavevector, \vec{k}_{spec} is the specular one and \vec{N} is the surface normal. The exact calculation is not difficult but becomes even simpler by taking into account that the detector is located far away from the target surface so that the variation of the location of the impact on the crystal surface can be neglected. We consider here that the beam impacts the surface exactly on its intersection with the rotation axis. Accordingly, the coordinates (y,z) on the detector depend only on the scattering angles. We only need to focus on the vector $\vec{N}(\phi)$ describing the surface normal tilted by an angle τ with respect to the rotation axis \vec{A} during azimuthal rotation ϕ around this axis. Defining the rotation around a vector \vec{u} by an angle α as $R_{\vec{u}}(\alpha)$, $\vec{N}(\phi)$ can be written as a product of three rotations describing the tilt angle $R_{\vec{y}}(\tau)$, the azimuthal scan $R_{\vec{z}}(\phi)$ and the angle of incidence θ_0 , $R_{\vec{y}}(\theta_0)$;

$$\vec{N}(\phi) = R_{\vec{y}}(\theta_0)R_{\vec{z}}(\phi)R_{\vec{y}}(\tau)\vec{z}$$

$$\vec{N}(\phi) = \begin{bmatrix} \cos \tau \sin \theta_0 + \cos \phi \cos \theta_0 \sin \tau \\ \sin \phi \sin \tau \\ \cos \tau \cos \theta_0 - \cos \phi \sin \tau \sin \theta_0 \end{bmatrix}$$

Considering for simplicity, unit vectors \vec{k}_{in} and \vec{k}_{out} , i.e. $k_0 = 1$, the scalar product $\vec{k}_{in} \cdot \vec{N}$ is the first coordinate of the vector \vec{N} so that, within Eq. (1), the y and z components of the specular wave-vector write;

$$k_y(\phi) = -2 \sin \phi \sin \tau (\cos \theta_0 \cos \phi \sin \tau - \sin \theta_0 \cos \tau)$$

$$k_z(\phi) = -2 \cos \tau (\cos \phi \cos \theta_0 \sin \tau - \sin \theta_0 \cos \tau)$$

with ϕ the azimuthal angle. For small angle θ_0 and τ the formula simplify and the coordinates $y(\phi), z(\phi)$ on the detector form the parametric equations of the orbit.

$$\begin{aligned} y(\phi) &= -2L\tau \sin \phi (\tau \cos \phi - \theta_0) \\ z(\phi) &= 2L\theta_0 - 2L\tau \cos \phi \end{aligned} \quad (2)$$

The Eq. (2) shows that the full vertical extension $W_z = 4L\tau$ and full width at half height $W_y = 4L\tau\theta_0$ are simple quantities while Fig. 2 illustrates that the orbits are not simple ellipses. (see Figs. 1 and 3)

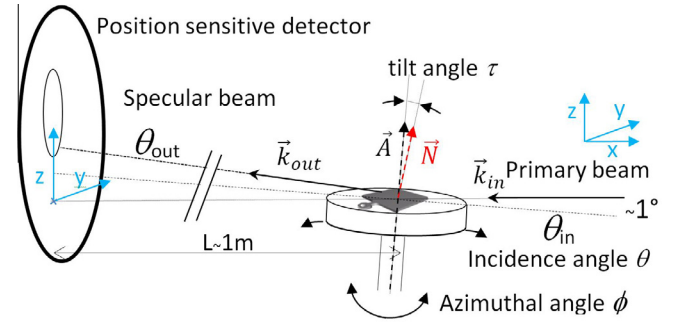


Fig. 1. Typical grazing incidence setup where the incident beam has a fixed direction. If the surface plane, defined here by its normal \vec{N} , is not exactly perpendicular to the rotation axis \vec{A} , the specular beam follows characteristic orbits during azimuthal scan.

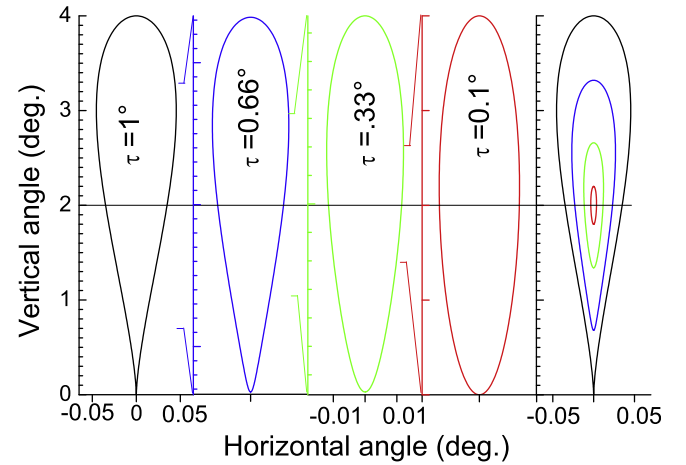


Fig. 2. Orbits corresponding to an angle of incidence $\theta_0 = 1^\circ$ and to a tilt angle τ of 1° , 0.66° , 0.33° and 0.1° . For each panel, the horizontal scale is zoomed \sim ten times compared with the vertical one. The rightmost panel plots the four orbits at the same scale.

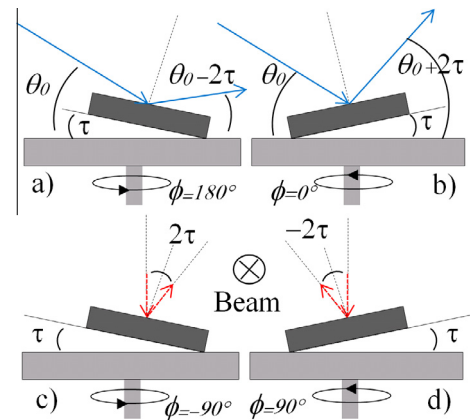


Fig. 3. The plane containing the rotation axis and the surface normal is plotted for four different azimuthal angles ϕ . Twice per revolution, at angles (b) $\phi = 0^\circ$ and (a) $\phi = 180^\circ$, this plane contains the primary beam, and coincides with the incidence plane. The outgoing angles differ by 4τ and the associated spots are separated by W_z . At 90° from these values, (c) and (d), the beam momentum \vec{k} is almost perpendicular to the reference plane with only a tiny component $k \sin \theta_0$ parallel to the rotation axis (in dashed red). In this projected plane, the variation in the deflection of the specular beam is again 4τ but the amplitude on the detector will only be $W_y = W_z \sin \theta_0$, i.e. almost two order of magnitude smaller than W_z . (For interpretation of the references to colour in this figure legend, the reader is referred to the web version of this article.)

Download English Version:

<https://daneshyari.com/en/article/1679525>

Download Persian Version:

<https://daneshyari.com/article/1679525>

[Daneshyari.com](https://daneshyari.com)